Struct Chem (2009) 20:399–407
DOI 10.1007/s11224-009-9424-1

ORIGINAL RESEARCH

Theoretical studies of a singlet oxygen-releasing dioxapaddlane (1,4-diicosa naphthalene-1,4-endoperoxide)

Alvaro Castillo · Alexander Greer

Received: 26 November 2008 / Accepted: 30 January 2009 / Published online: 17 March 2009

Abstract Theoretical calculations have been used to examine singlet oxygen release from a naphthalene endoperoxide which bears a flexible $(CH_2)_{22}$ polymethylene "lid". Monte Carlo and ONIOM calculations that incorporated semi-empirical and density functional theory predicted the conformational influence of the polymethylene chain in the cycloreversion of dioxapaddlane, 1,4-diicosa naphthalene-1,4-endoperoxide, to $^1O_2$ and 1,4-diicosa naphthalene. This study attempts to build a connection between $^1O_2$ generation and "jump rope" dynamics of the dioxapaddlane. The polymethylene chain appears to function as a gatekeeper for the oxygen. Instead of coming full circle, a semi-circle rotation of the polymethylene bridge protected the peroxide group, limiting the dissociation of $^1O_2$ from the naphthalene site.

Keywords Singlet oxygen · Naphthalene endoperoxide · Jump rope dynamics · Paddlane

Introduction

1,4-Dimethyl naphthalene (**1**) reversibly binds $^1O_2$; upon heating, the naphthalene endoperoxide (**2**) dissociates into $^1O_2$ and a small amount of $^3O_2$ (Scheme 1) [1]. Modifications of substituents at the 1,4-positions of naphthalene have been made [2–8]. Naphthalene **3** has bulky substituents slowing the rate of $^1O_2$ addition at the 1,4-positions so that binding at the 6,9-positions also took place [9–10]. For an example of a tetracene system see [11]. Singlet oxygen release has also been examined in polymeric endoperoxides [12–19] such as 1,4-dimethyl-2-poly(vinylnaphthalene-1,4-endoperoxide) [19]. But no studies have yet focused on the $^1O_2$ release from a naphthalene endoperoxide molecule bearing a "lid". Computational methods can be applied to such a problem; however, such studies remain highly challenging. Owing to its multiconfigurational character, computational studies on $^1O_2$ with compounds containing 10 or more carbon atoms are rather uncommon [20–30]. Encouragingly, Wasserman et al. [31] showed that B3LYP/6-311+G(d) calculations reproduced the experimental energetics of several naphthalene-$^1O_2$/naphthalene endoperoxide pairs—including compounds **1** and **2**. Due to the success of the study of Wasserman et al. [31], one may anticipate that replacing the methyls at the 1,4-positions with a polymethylene bridge would be amenable to computation [e.g., 1,4-diicosa naphthalene (**5**) and 1,4-diicosa naphthalene-1,4-endoperoxide (**6**)] (Scheme 2).

Researchers have examined polymethylene-bridged molecules for many years [32–43]. The length and anchor position of the polymethylene chain can expose or "hide" a reactive site of a compound (Scheme 3). In 1980, Busch et al. [44, 45] showed that the chain of length six (rather than five) methylenes increased the affinity of oxygen in cobalt cyclidene **7**, which formed a CoO_2 adduct. In 1980, Marshall [32] showed that unlike *trans*-fused **9**, *cis*-fused **8** forms a colored charge-transfer complex with tetracyanoethylene (TCNE) due to its less shielded alkene site. Another intriguing class of polymethylene-bridged compounds are paddlanes, such as structures **10**–**12** [46–56]. Theoretical calculations yielded valuable information on

Dedicated to István Hargittai for his first twenty years at *Structural Chemistry*.

A. Castillo · A. Greer (✉)
Department of Chemistry and Graduate Center, Brooklyn College, The City University of New York (CUNY), Brooklyn, NY 11210, USA
e-mail: agreer@brooklyn.cuny.edu

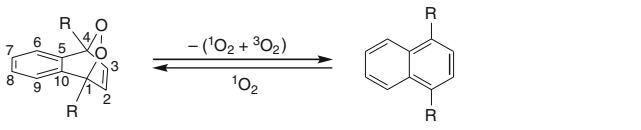

2 (R=CH_3) **1** (R=CH_3)

4 (R=$CH(CONHCH_2CH_2(OH)CH_2OH)_2$) **3** (R=$CH(CONHCH_2CH_2(OH)CH_2OH)_2$)

Scheme 1 Reaction of 1,4-disubstituted naphthalenes with singlet oxygen

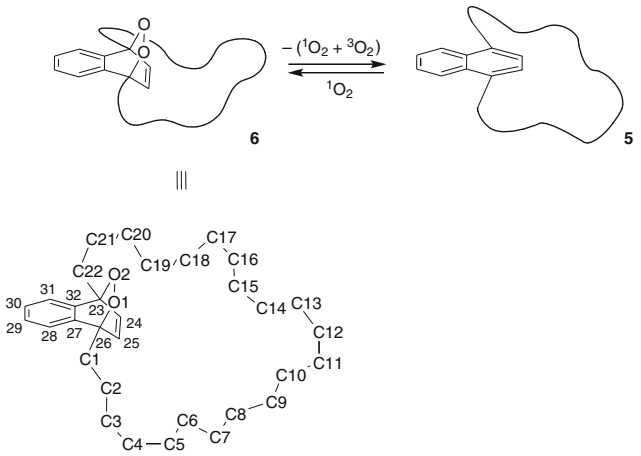

Scheme 2 Release of singlet oxygen from 1,4-diicosa naphthalene-1,4-endoperoxide

Scheme 3 Compounds which contain polymethylene bridges

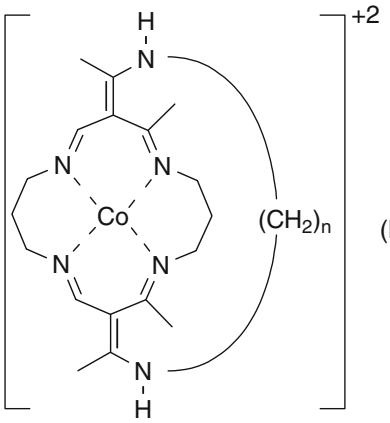

7 axial N-methylimidazole not shown

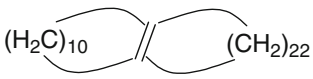

8

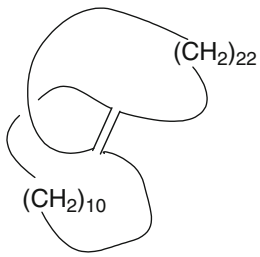

9

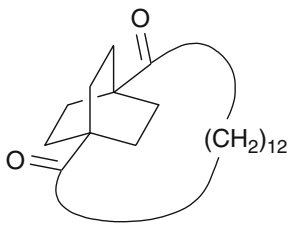

10

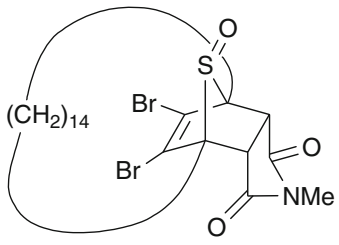

11

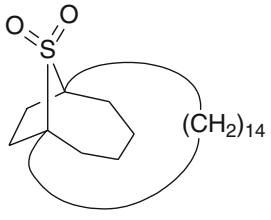

12 synthesis attempted

the reactivity and conformational properties of polymethylene-bridged compounds [57–61] and paddlanes [62–64].

Here, we present results of Monte Carlo and ONIOM calculations that incorporated AM1 and B3LYP to analyze the conformational influence of the polymethylene chain in the cycloreversion of **6**, yielding $^1O_2$ and **5**. The **5/6** pair was selected because the polymethylene chain was sufficiently long, that it could undergo rope-skipping conformational changes on the basis of Dreiding models creating a possible O_2 binding site at the 23,26-positions (Scheme 2). Binding or release of $^1O_2$ at the 28,31-positions was not computed. The idea was that chain rotation (full-circle versus semi-circle) might lead to increased endoperoxide stability at higher temperatures based on an increased rate of rotation, which led us enquire into a possible oxygen "gatekeeper" mechanism.

Computational details

Semi-empirical and density functional theoretical (DFT) calculations were conducted with the Gaussian 03 program package [65]. Monte Carlo calculations were conducted with Hyperchem 8.0 (Hypercube, Inc., Gainesville, Fl). Standard computational protocols were used [66] and the

structures were viewed with the GaussView program [67]. A previous computational study demonstrated that the 6-311+G* basis set adequately described the naphthalene endoperoxide decomposition reaction surface [31]. The transition state structures **TS-AM1** and **TS-B3LYP**, and those connecting the pairs **5/6**, **13/14**, **15/16**, and **17/18** were confirmed to be transition states by frequency calculations and by conducting internal reaction coordinate (IRC) calculations for the reaction path for the transition (Fig. 1 and Table 1). IRC calculations were not performed on the ONIOM derived transitions state structures. Conformations of **6** were searched by the Monte Carlo method with the MM+ force field. The MM+ calculations were followed by AM1 optimizations with the Fletcher–Reeves conjugate gradient algorithm and the lowest energy conformations reoptimized by ONIOM(B3LYP/6-311+G*:AM1). **6TSa/b**, **6TSb/c**, **6TSc/d**, **6TSd/e**, and **6TSe/a** were assumed to be transition state structures, since they cannot be examined by IRC calculations. All energetics obtained were corrected for zero-point energies (ZPE). The ONIOM treatment separated the lid from the rest of the molecule, in which the junction between

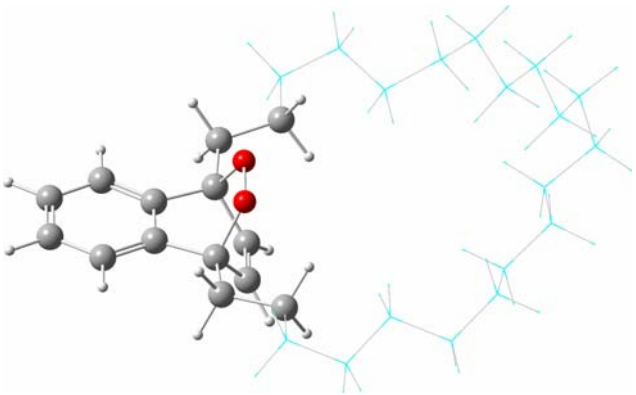

Scheme 4 The DFT portion of the ONIOM calculation is shown with a ball-and-stick model, and the AM1 portion is shown with a wireframe model

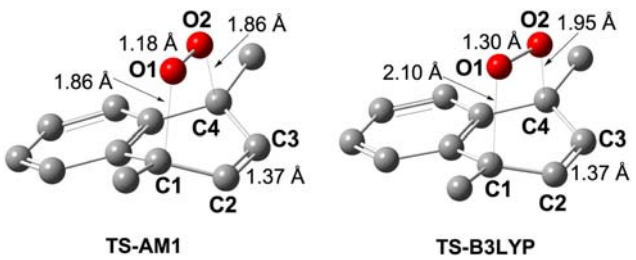

Fig. 1 AM1 optimized (*left*) and B3LYP/6-311+G* optimized (*right*) transition state structures for the decomposition of 1,4-dimethyl-1,4-naphthalene endoperoxide **2** to 1,4-dimethyl naphthalene **1** and $^1O_2$. For clarity, the hydrogens are not shown

B3LYP/6-311+G* and AM1 was at the C(2)–C(3) and C(20)–C(21) bonds (cf. Schemes 2 and 4).

Results and discussion

Singlet oxygen release from endoperoxides

Our first aim was to evaluate whether naphthalene endoperoxide decompositions could be accurately computed with the fairly low-cost computational methods B3LYP/6-311+G*//AM1 and ONIOM(B3LYP/6-311+G*:AM1). Our paper builds on Wasserman's previous DFT study of naphthalene endoperoxides, in which the B3LYP/6-311+G* energy of $^1O_2$ was estimated to be −150.30756 Hartrees [31]. AM1 and B3LYP/6-311+G* transition state structures (TSs) corresponding to the decomposition of naphthalene endoperoxide **2** to naphthalene **1** and $^1O_2$ are shown in Fig. 1. **TS-AM1** has a shorter C(1)–O(1) bond (0.24 Å), C(4)–O(2) bond (0.09 Å), and O(1)–O(2) bond (0.12 Å) compared to **TS-B3LYP**, and the O(2)–O(1)–C(1)–C(2) torsion angle is 18° larger [cf. 58° (**TS-AM1**) vs. 40° (**TS-B3LYP**)]. Similar transition structure geometries were found for $^1O_2$ dissociation from 1,4-diicosa naphthalene-1,4-endoperoxide **6**, naphthalene-1,4-endoperoxide **14**, 1-ethylnaphthalene-1,4-endoperoxide **16**, and 1,4,5-trimethylnaphthalene-1,4-endoperoxide **18**.

The decomposition of naphthalene endoperoxides is reminiscent of retro Diels–Alder reactions of "masked" dienes (Scheme 5) [68–71]. Masked dienes such as compound **19** are similar to the naphthalene compounds studied here, in which DFT methods often yield results in excellent agreement with experiment [68–74]; although, the B3LYP functional is not devoid of shortcomings especially with larger sized molecules [75, 76]. We find the decomposition of endoperoxides **2**, **6**, **14**, **16**, and **18** to be endothermic by 6–17 kcal/mol (Table 1). The energy of **2** relative to **1** and $^1O_2$ was similar with B3LYP/6-311+G* (11 kcal/mol) and B3LYP/6-311+G*//AM1 (13 kcal/mol) calculations. The activation energy barriers for the release of $^1O_2$ from the endoperoxides ranged from 20 to 28 kcal/mol. The B3LYP/6-311+G*//AM1 structure **TS-AM1** (25 kcal/mol) was predicted to be 4 kcal/mol higher in energy than the B3LYP/6-311+G* structure **TS-B3LYP** (21 kcal/mol) for the reaction of **2** to **1** and $^1O_2$. The computed barrier

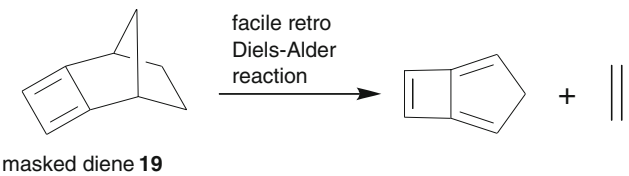

Scheme 5 A retro Diels-Alder reaction of a masked diene

Table 1 Calculated and experimental energetics for decomposition reactions of endoperoxides

Reaction	$\Delta E^{\ddagger}$ (kcal/mol)			$\Delta G^{\ddagger}$ exptl. (kcal/mol)[g]	ΔE (kcal/mol)		
	B3LYP[a,d]	B3LYP //AM1[b,d]	ONIOM[c]		B3LYP[a,d]	B3LYP //AM1[b,d]	ONIOM[c]
A 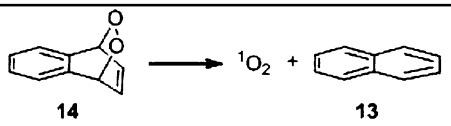 **14** **13**	21	26	–	–	6	6	–
B 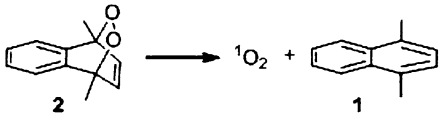 **2** **1**	21	25	–	23.6	11	13	–
C[e] 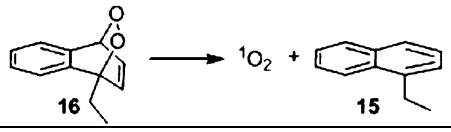 **16** **15**	20	25	22	–	10	9	6
D 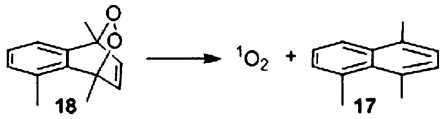 **18** **17**	21	26	–	25.9	14	17	–
E 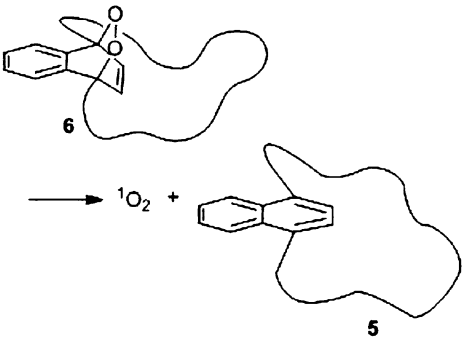 **6** **5**	–	28[f]	22[f]	–	–	10	15

[a] B3LYP/6-311+G*

[b] B3LYP/6-311+G*//AM1

[c] ONIOM(B3LYP/6-311+G*:AM1)

[d] The B3LYP/6-311+G* energy of $^1O_2$ is −150.30756 Hartrees (Ref. [31])

[e] Reaction C reports values for the "out" conformer of 1-ethylnaphthalene-1,4-endoperoxide **16**, which is more stable than the "in" conformer by 0.2 kcal/mol

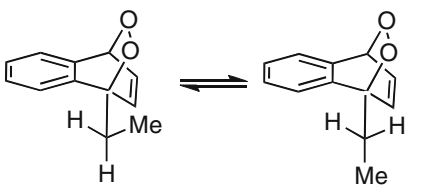

"out" conformer **16** "in" conformer **16**

[f] The global minima for 1,4-diicosa naphthalene **5** and 1,4-diicosa naphthalene-1,4-endoperoxide **6** were found based on a Monte Carlo conformational search of the potential energy surface with the MM+ force field and reoptimization of the lowest energy conformers by ONIOM(B3LYP/6-311+G*:AM1)

[g] Ref. [31]

heights are similar to the experimental free energy barriers [cf. experimental value of **2** ($\Delta G^{\ddagger} = 23.6$ kcal/mol) with B3LYP/6-311+G*//AM1 ($\Delta E^{\ddagger} = 25$ kcal/mol), and the experimental value of **17** ($\Delta G^{\ddagger} = 25.9$ kcal/mol) with B3LYP/6-311+G*//AM1 ($\Delta E^{\ddagger} = 26$ kcal/mol)]. ONIOM(B3LYP/6-311+G*:AM1) produces an activation energy of 22 kcal/mol when the junction between B3LYP and AM1 was situated at the methyl and methylene carbon atoms in the **15/16** pair (Reaction C, Table 1). The qualities of the energetics of the B3LYP/6-311+G*//AM1 and ONIOM(B3LYP/6-311+G*:AM1) calculations were very good compared with those obtained with B3LYP/6-311+G* and experimental observations [31]. The data suggested that naphthalene endoperoxide decompositions can be computed to within ±3 kcal/mol with B3LYP/6-311+G*//AM1 for **2**, **14**, **16**, and **18**, and ONIOM(B3LYP/6-311+G*:AM1) for **6** and **16**.

Conformational analysis of "jump rope" endoperoxide **6**

Our second aim was to compute the lowest energy path for **6** corresponding to a 360° circular rotation of the polymethylene chain around the endoperoxide core. Endoperoxide **6** is an example of a paddlane, where the fused benzene and peroxide groups are rigid, and the polymethylene chain is very flexible. Conformations of **6** were searched by the Monte Carlo method with the MM+ force field followed by AM1 optimizations. The dihedral angle θ = C(25)–C(26)–C(1)–C(2) was followed in 10° increments and the dihedral angle ϕ = C(24)–C(23)–C(22)–C(21) was followed in 15° increments, each independently, for the 360° rotation of the rope (i.e., 36 × 24 grid) (Fig. 2). The dihedral angle θ is positive for a counter clockwise movement from C(2) to C(25) as one looks from C(1) to C(26). The ϕ dihedral angle is positive for a counter clockwise movement from C(21) to C(24) as one looks from C(23) to C(22). Due to the high flexibility of the polymethylene chain, each of the 864 points on the 36 × 24 grid (not surprisingly) possessed thousands of conformations. For example, **6a** was found from a search of 4456 conformations, which arose from an initial geometry that was chosen to have the polymethylene group facing *anti* to the fused benzene ring. Thus, restrictions were applied to obtain a rough estimation as to the nature of the conformational potential energy surface. Cutoff criteria were used where each of the 864 points on the 36 × 24 grid was limited to 10,000 optimizations and a rejection criteria of 6 kcal/mol. This cutoff criteria led to the generation of ~200 conformations for each of the 864 points. The resulting lowest energy conformation from these ~200 conformations was optimized by AM1 and then reoptimized by ONIOM(B3LYP/6-311+G*:AM1).

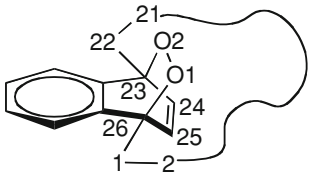

6a

The lowest energy pathway for the 360° rotation of the polymethylene chain in **6** was deduced from the three-dimensional plot in Fig. 2. Figure 3 shows the most important geometries, in which conformers are displayed in side-on views. The jump rope rotation process is not particularly remarkable. As expected, we find that **6a** is the global minimum, in which the polymethylene chain is *anti* to the largest of the three paddles of the paddlane, the fused benzene ring. The torsion angles optimized for **6a** were $\theta = 54°$ and $\phi = 60°$. A transition state has been located (**6TSa/b**) connecting **6a** with **6b**, which predicts the C(23)–O(2) bond eclipses the C(21)–C(22) bond, in which $\theta = 59°$ and $\phi = 120°$. The activation barrier of **6TSa/b** is 4 kcal/mol. Rotamer **6b** has the C(22)–C(23) connector bond *gauche* to the peroxide and alkene, the C(1)–C(26) connector bond *gauche* to the fused benzene and alkene. Rotamer **6b′** has the C(1)–C(26) connector bond *gauche* to the peroxide and alkene, and the C(22)–C(23) connector bond *gauche* to the fused benzene and alkene. Rotamers **6b** and **6b′** led to **6c**. Transition state **6TSb/c** predicted that the C(26)–O(1) is eclipsed by the C(1)–C(2) bond, in which $\theta = 120°$ and $\phi = 166°$. In minimum **6c**, the polymethylene chain is situated *anti* to the alkene group, here with $\theta = 160°$ and $\phi = 167°$. Transition state **6TSc/d**

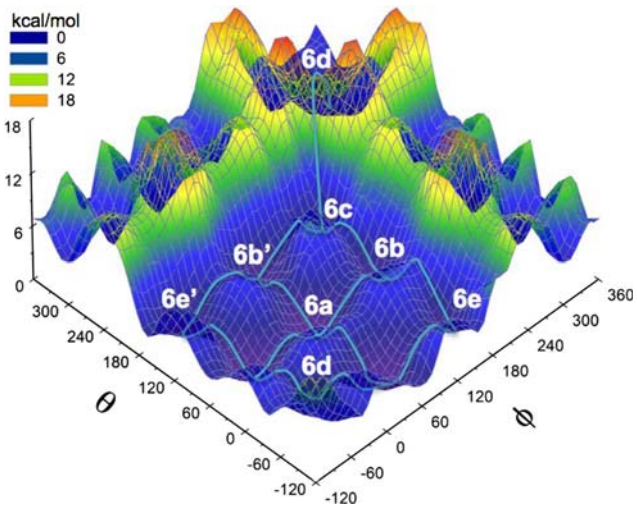

Fig. 2 Three-dimensional computed energy plot for the rotation of the polymethylene chain in **6**

represents the polymethylene chain passing over the fused benzene ring and was the highest point on the PES (17 kcal/mol, Fig. 3) due to a repulsive steric interaction between the benzene hydrogens and the methylene hydrogens. Rotamer **6d** has the polymethylene chain *anti* to the peroxide group. Transition state **6TSd/e** has the C(1)–C(2) and C(25)–C(26) bonds eclipsed, in which with $\theta = 0°$ and $\phi = 56°$. Rotamer **6e** has the C(1)–C(26) connecting point of the chain *gauche* to the peroxide and alkene, the C(22)–C(23) connecting point of the chain *gauche* to the fused benzene and alkene. Rotamer **6e′** has the C(22)–C(23) connecting point of the chain *gauche* to the peroxide and alkene, and the C(1)−C(6) connecting point of the chain *gauche* to the fused benzene and alkene. Transition state **6TSe/a** connects **6e** with **6a**, in which the activation barrier is 5 kcal/mol where $\theta = 49°$ and $\phi = 0°$.

The two-layered ONIOM approach using DFT and semiempirical theory often performs well and supports experimental findings [77–80]. Nonetheless, our Monte Carlo and ONIOM approach was further investigated to determine whether it would successfully reproduce the experimental energetics of a test compound, dioxa-1,5-naphthalenophane (**19**), which involved a 180° rotation in a "jump rope" enantiomerization reaction (Fig. 4) [58, 59]. The dihedral angles θ = O(2)–C(15)–C(14)–C(13) and ϕ = C(20)–C(21)–O(1)–C(1) were followed in 20° increments, each independently, for the 360° rotation of the rope

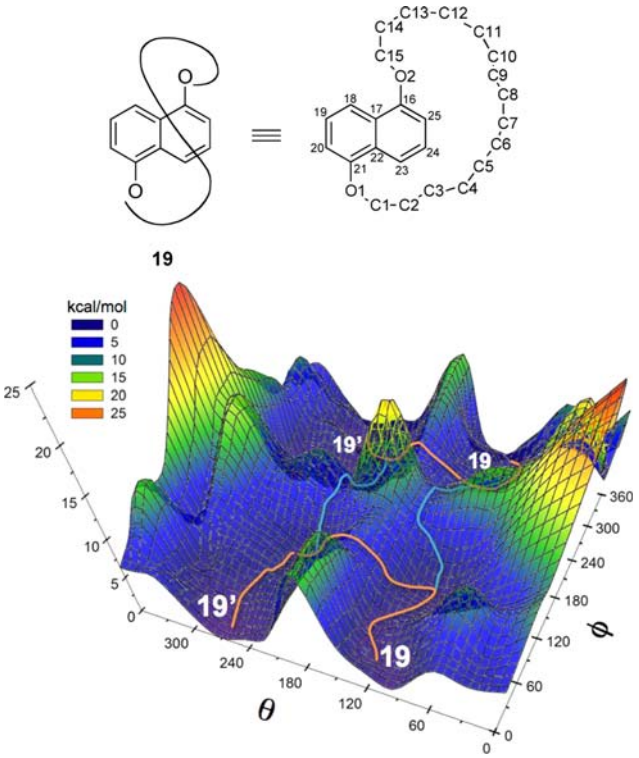

Fig. 4 Three-dimensional computed energy plot for the 180° rotation of the polymethylene chain in **19**. Orange lines represent pathways to enantiomerizations. *Blue lines* represent the full-circle rotation of the polymethylene chain

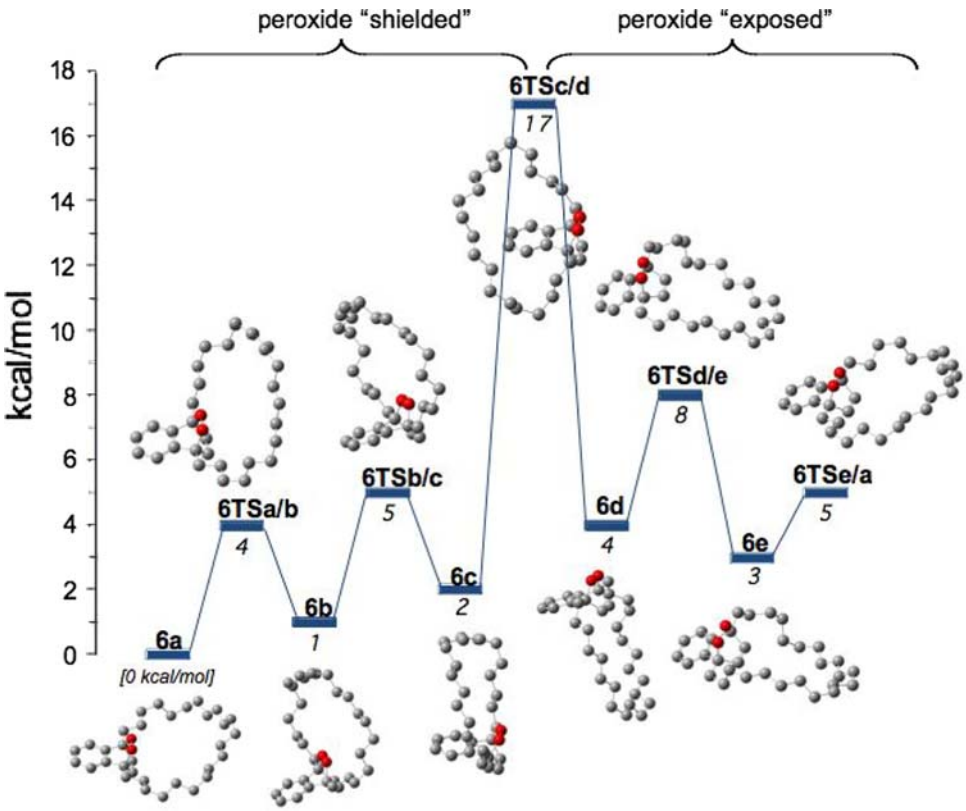

Fig. 3 Side-on views of geometries and the conformational variations for the lowest energy path for rotation of the polymethylene chain of **6** in a counterclockwise direction. The peroxide group (*red*) is connected to carbon atoms (*gray*) where the naphthalene and polymethlyene attach. The hydrogen atoms are not shown. The lowest energy conformations were obtained by HyperChem and reoptimized at the ONIOM(B3LYP/6-311+G*:AM1) level

(i.e., 19 × 19 grid). Cutoff criteria were used (similar to that for **6**) where each of the 361 points yielded ~200 conformations, in which the lowest in energy was optimized by AM1 and then reoptimized by ONIOM(B3LYP/6-311+G*:AM1). The dihedral angle θ is positive for a clockwise movement from C(20) to C(1) as one looks from C(21) to O(1). The ϕ dihedral angle is positive for a clockwise movement from O(2) to C(13) as one looks from C(15) to C(14). The transition structure connecting **19** with **19′** on the front portion of the figure contained $\phi = 117°$ and $\theta = 162°$. A similar transition structure can be found at the back portion of the figure, which represents an approximate mirror image of the first transition structure. This Monte Carlo and ONIOM treatment resulted in an activation energy ($\Delta E^{\ddagger} = 6$ kcal/mol) for a 180° rotation of the jump rope in **19**, which was similar with the experimental enantiomerization process measured to be 7.6 ± 0.8 kcal/mol [58, 59]. Even though the reproduction of the experimental enantiomerization barrier in **19** was successful, the conformational search on endoperoxide **6** may miss some details. For example, there was no guarantee that the minima found at each step were accessible in a continuous revolution of the angles on the 36 × 24 grid. The 22 C atoms in the ring have ~60 heavy-atom vibrational modes, in which the hydrogen atoms are assumed not to affect the matter substantially. Thus, 10,000 Monte Carlo steps may be sufficient to find a minimum if the structure is well-behaved; that is, in a simpler system relative to a structure such as **6**, which had a significant number of local minima.

Effect of the polymethylene lid on $^1O_2$ formation

Our third aim was to examine the influence of chain rotation of **6** with the unimolecular formation of $^1O_2$ and **5**. The calculations determined conformational stability of **6** based on the position of the polymethylene bridge and a trend for dissociation of $^1O_2$ with the "active" forms **6d**, **6e**, **6a** ≫ **6b**, **6c** appearing in different order compared to conformer stability **6a** > **6b** > **6c** > **6e** > **6d**. ONIOM saddle points like the one connecting **6** with **5** and $^1O_2$ have been located for conformers **6a**, **6d**, and **6e**. Attempts at transition state optimizations for **6b** and **6c** resulted in rotation of the polymethylene bridge away from the dissociating $^1O_2$ site. Only those conformations that did not have the polymethylene lid situated over the peroxide group readily decomposed to $^1O_2$ and **5**. For example, rotamer **6d** had the polymethylene lid *gauche* to the benzene and ethylene groups so the peroxide group is highly exposed. Due to the low rotation energies connecting conformers **6a–6e** via **6TSa/b**, **6TSb/c**, **6TSd/e**, and **6TSe/a**, we postulate that the polymethylene chain functions as a gatekeeper for the oxygen, protecting the peroxide moiety, and potentially limiting the dissociation of $^1O_2$ from the naphthalene site.

The B3LYP/6-311+G*//AM1 activation energy for the dissociation of $^1O_2$ from **6a** ($\Delta E^{\ddagger} = 28$ kcal/mol) was predicted to be higher for **2** ($\Delta E^{\ddagger} = 25$ kcal/mol), but the ONIOM(B3LYP/6-311+G*:AM1) activation energy for **6a** was found to be lower ($\Delta E^{\ddagger} = 22$ kcal/mol), but no trend emerges (Table 1). Naphthalene **5** may reversibly bind $^1O_2$, and while this process was not modeled, one may expect that the jump rope substituent at the 23,26-positions of naphthalene would slow the rate of $^1O_2$ addition to **5** so that competitive binding of $^1O_2$ at the 28,31-positions could also take place [9–11]. Reiterating a point made in the Introduction, the bulky maloamide substitutents in **3** are known to exert steric interactions that slowed binding of $^1O_2$ at the 1,4-positions, binding of $^1O_2$ at the 6,9-positions in a ratio of ~1:100 (1,4:6,9).

Conclusion

Our computational examination of a hypothetical $^1O_2$-carrier **6** was inspired by rope-skipping molecules that have been the subject of study for over 30 years [32–61]. The qualities of the energetics of $^1O_2$ dissociation from naphthalene endoperoxides with B3LYP/6-311+G*//AM1 and ONIOM(B3LYP/6-311+G*:AM1) were very good compared with those obtained with B3LYP/6-311+G* and experimental observations [1, 31]. The energetics of $^1O_2$ dissociation from the naphthalene site can only be tentatively determined in relation to the position of the $(CH_2)_{22}$ polymethylene lid due to the need for improved models that can compute the dynamics of the lid and the extent of chain clearance required in the singlet oxygen release process. Conformers **6b–6e** were 4 kcal/mol or less above the global minimum **6a**, and the polymethylene chain favored semi-circle rotation where the ability to dissociate $^1O_2$ from conformers **6b** and **6c** was diminished due to shielding. In a similar vein, a large body of literature is available for $^1O_2$ generation, and a growing fraction of it is focusing on the escape of $^1O_2$ from confined and shielded environments [81–87].

Acknowledgments We thank the NIH (S06 GM076168-01) and the PSC-CUNY Grants Program for support. Computational support was provided by the CUNY Graduate Center computational facility. We thank Prof. Mark Kobrak for stimulating discussions.

References

1. Wasserman HH, Larsen DL (1972) Chem Commun 5:253
2. Aubry J-M, Pierlot C, Rigaudy J, Schmidt R (2003) Acc Chem Res 36:668. doi:10.1021/ar010086g

3. Saito I, Matsuura T (1979) In: Wasserman HH, Murray RW (eds) Singlet oxygen, vol 40. Academic Press, New York, p 511
4. Balci M (1981) Chem Rev 81:91. doi:10.1021/cr00041a005
5. Clennan EL, Foote CS (1992) In: Ando W (ed) Organic peroxides. Wiley, Chichester, UK, p 255
6. Turro NJ, Chow MF, Rigaudy J (1981) J Am Chem Soc 103:7218. doi:10.1021/ja00414a029
7. Ben-Shabat S, Itagaki Y, Jockusch S, Sparrow JR, Turro NJ (2002) Angew Chem Int Ed Engl 41:814. doi:10.1002/1521-3773(20020301)41:5<814::AID-ANIE814>3.0.CO;2-2
8. Aubry J-M, Mandard-Cazin B, Rougee M, Bensasson RV (1995) J Am Chem Soc 117:9159. doi:10.1021/ja00141a006
9. Pierlot C, Aubry J-M (1997) Chem Commun (Camb) 38:2289. doi:10.1039/a705716d
10. Pierlot C, Poprawski J, Marko J, Aubry J-M (2000) Tetrahedron Lett 41:5063
11. Liang Z, Zhao W, Wang S, Tang Q, Lam S-C, Miao Q (2008) Org Lett 10:2007
12. Saito I, Nagata R, Matsuura T (1981) Tetrahedron Lett 22:4231. doi:10.1016/S0040-4039(01)82112-2
13. Twarowski A (1988) J Phys Chem 92:6580. doi:10.1021/j100334a021
14. Wixom MR (1990) J Phys Chem 94:4926. doi:10.1021/j100375a031
15. Fudickar W, Linker T (2006) Chem Eur J 12:9276
16. Zehm D, Fudickar W, Linker T (2007) Angew Chem Int Ed 46:7689
17. Sheats JR (1992) Trends Phys Chem 3:191
18. Mondal R, Shah BK, Neckers DC (2007) J Photochem Photobiol A: Chem 192:36
19. Twarowski A, Dao P (1988) J Phys Chem 92:5292. doi:10.1021/j100329a045
20. Garavelli M, Bernardi F, Olivucci M, Robb MA (1998) J Am Chem Soc 120:10210. doi:10.1021/ja9805270
21. Bobrowski M, Liwo A, Oldzieg S, Jeziorek D, Ossowski T (2000) J Am Chem Soc 122:8112. doi:10.1021/ja001185c
22. Sevin F, McKee ML (2001) J Am Chem Soc 123:4591. doi:10.1021/ja010138x
23. Langeland JL, Werstiuk NH (2003) Can J Chem 81:525. doi:10.1139/v03-037
24. Singleton DA, Hang C, Szymanski MJ, Meyer MP, Leach AG, Kuwata KT, Chen JS, Greer A, Foote CS, Houk KN (2003) J Am Chem Soc 125:1319. doi:10.1021/ja027225p
25. Ricca A, Bauschlicher CW (2003) Phys Rev B 68:035433. doi:10.1103/PhysRevB.68.035433
26. Y-f Zhang, Z-f Liu (2004) J Phys Chem B 108:11435. doi:10.1021/jp049088j
27. Yim WL, Liu ZF (2004) Chem Phys Lett 398:298. doi:10.1016/j.cplett.2004.09.082
28. Paterson MJ, Christiansen O, Jensen F, Ogilby PR (2006) Photochem Photobiol 82:1136. doi:10.1562/2006-03-17-IR-851
29. Burgert R, Schnöckel H, Grubisic A, Li X, Stokes ST, Bowen KT, Ganteför GF, Kiran B, Jena P (2008) Science 319:438. doi:10.1126/science.1148643
30. Leach AG, Houk KN, Foote CS (2008) J Org Chem 73:8511. doi:10.1021/jo8016154
31. Wasserman HH, Wiberg KB, Larsen DL, Parr J (2005) J Org Chem 70:105. doi:10.1021/jo040228v
32. Marshall JA (1980) Acc Chem Res 13:213. doi:10.1021/ar50151a004
33. Marshall JA (1989) Chem Rev 89:150. doi:10.1021/cr00097a006
34. Busch DH, Alcock NW (1994) Chem Rev 94:585. doi:10.1021/cr00027a003
35. Winnik MA (1981) Chem Rev 81:491. doi:10.1021/cr00045a004
36. Dale J (1976) Top Stereochem 9:199
37. Kanomata N, Ochiai Y (2001) Tetrahedron Lett 42:1045
38. Whitlock BJ, Whitlock HW (1983) J Am Chem Soc 105:838. doi:10.1021/ja00342a032
39. Paquette LA, Trova MP (1988) J Am Chem Soc 110:8197. doi:10.1021/ja00232a037
40. Marshall JA, Audia VH, Jenson TM, Guida WC (1986) Tetrahedron 42:1703. doi:10.1016/S0040-4020(01)87587-6
41. Fraser SJ, Winnik MA (1981) J Chem Phys 75:4683. doi:10.1063/1.442586
42. Ueda T, Kanomata N, Machida H (2005) Org Lett 7:2365. doi:10.1021/ol0506258
43. Inoue Y, Ueoka T, Kuroda T, Hakushi T (1983) J Chem Soc, Perkin Trans 2 7:983. doi:10.1039/p29830000983
44. Stevens JC, Busch DH (1980) J Am Chem Soc 102:3285. doi:10.1021/ja00529a084
45. Lin W-K, Alcock NW, Busch DH (1991) J Am Chem Soc 113:7603. doi:10.1021/ja00020a023
46. Eaton PE, Leipzig BD (1983) J Am Chem Soc 105:1656. doi:10.1021/ja00344a042
47. Li YQ, Thiemann T, Mimura K, Sawada T, Mataka S, Tashiro M (1998) Eur J Org Chem 9:1841. doi:10.1002/(SICI)1099-0690(199809)1998:9<1841::AID-EJOC1841>3.0.CO;2-P
48. Paquette LA, Fabris F, Tae J, Gallucci JC, Hofferberth JE (2000) J Am Chem Soc 122:3391. doi:10.1021/ja9943849
49. Paquette LA, Mendez-Andino J (2001) Tetrahedron Lett 42:967. doi:10.1016/S0040-4039(00)02212-7
50. Tobe Y, Fujita H, Wakaki I, Terashima K, Kobiro K, Kakiuchi K, Odaira Y (1984) J Chem Soc Perkin Trans 1 12:2681. doi:10.1039/p19840002681
51. Newkome GR, Theriot KJ, Gupta VK, Balz RN, Fronczek FR (1986) Inorg Chim Acta 114:21. doi:10.1016/S0020-1693(00)84582-X
52. Wada Y, Ishimura T, Nishimura (1992) J Chem Ber 125:2155. doi:10.1002/cber.19921250926
53. Schwartz MH, Rosenfeld SM, Lee CI, Jasinski JP, Dardon EH (1992) Tetrahedron Lett 33:6275. doi:10.1016/S0040-4039(00)60951-6
54. Inokuma S, Gao S-R, Nishimura (1995) J Chem Lett 8:689. doi:10.1246/cl.1995.689
55. Nakamura Y, Hayashida Y, Wada Y, Nishimura J (1997) Tetrahedron 53:4593. doi:10.1016/S0040-4020(97)00171-3
56. Elk SB (1987) J Chem Inf Comput Sci 27:70. doi:10.1021/ci00054a006
57. Davis WM, Zask A, Nakanishi K, Lippard SJ (1985) Inorg Chem 24:3737. doi:10.1021/ic00217a009
58. Chang MH, Masek BB, Dougherty DA (1985) J Am Chem Soc 107:1124. doi:10.1021/ja00291a007
59. Masek BB, Santarsiero BD, Dougherty DA (1987) J Am Chem Soc 109:4373. doi:10.1021/ja00248a039
60. Cort AD, Mandolini L, Pasquini C, Schiaffino L (2005) J Org Chem 70:9814. doi:10.1021/jo0515430
61. Brown AB, Whitlock HW (1989) J Am Chem Soc 111:3640. doi:10.1021/ja00192a023
62. Dodzuik H, Leszczynski J, Nowinski KS (1997) J Mol Struct Theochem 391:201. doi:10.1016/S0166-1280(96)04801-4
63. Würthwein EU, Chandrasekhar J, Jenmis ED, Schleyer Pv R (1981) Tetrahedron Lett 22:843. doi:10.1016/0040-4039(81)80011-1
64. Wiberg KB (1985) Tetrahedron Lett 26:5967. doi:10.1016/S0040-4039(00)98273-X
65. Frisch MJ, Trucks GW, Schlegel HB, Scuseria GE, Robb MA, Cheeseman JR, Montgomery JA Jr, Vreven T, Kudin KN, Burant JC, Millam JM, Iyengar SS, Tomasi J, Barone V, Mennucci B, Cossi M, Scalmani G, Rega N, Petersson GA, Nakatsuji H, Hada M, Ehara M, Toyota K, Fukuda R, Hasegawa J, Ishida M, Nakajima T, Honda Y, Kitao O, Nakai H, Klene M, Li X, Knox JE, Hratchian HP, Cross JB, Adamo C, Jaramillo J, Gomperts R,

Stratmann RE, Yazyev O, Austin AJ, Cammi R, Pomelli C, Ochterski JW, Ayala PY, Morokuma K, Voth GA, Salvador P, Dannenberg JJ, Zakrzewski VG, Dapprich S, Daniels AD, Strain MC, Farkas O, Malick DK, Rabuck AD, Raghavachari K, Foresman JB, Ortiz JV, Cui Q, Baboul AG, Clifford S, Cioslowski J, Stefanov BB, Liu G, Liashenko A, Piskorz P, Komaromi I, Martin RL, Fox DJ, Keith T, Al-Laham MA, Peng CY, Nanayakkara A, Challacombe M, Gill PMW, Johnson B, Chen W, Wong MW, Gonzalez C, Pople JA (2003) Gaussian 03, Revision D.01, Gaussian, Inc., Wallingford CT

66. Jensen F (2007) Introduction to computational chemistry. Wiley & Sons, Chichester, UK
67. Dennington RII, Keith T, Millam J (2007) GaussView, Version 4.1. Semichem, Inc., Shawnee Mission, KS
68. Dinadayalane TC, Sastry GN (2002) J Chem Soc Perkin Trans 2 11:1902. doi:10.1039/b205663a
69. Punnagai M, Dinadayalane TC, Sastry GN (2004) J Phys Org Chem 17:152. doi:10.1002/poc.707
70. Dinadayalane TC, Punnagai M, Sastry GN (2003) J Mol Struct 626:247
71. Geetha K, Dinadayalane TC, Sastry GN (2003) J Phys Org Chem 16:298. doi:10.1002/poc.615
72. Leach AG, Houk KN, Reymond J-L (2004) J Org Chem 69:3683. doi:10.1021/jo035669d
73. Beno BR, Wilsey S, Houk KN (1999) J Am Chem Soc 121:4816. doi:10.1021/ja9818250
74. Tantillo DJ, Lee JK (2007) Annual Rep Prog Chem Sect B Org Chem 103:272
75. Wodrich MD, Corminboeuf C, Schreiner PR, Fokin AA, Schleyer PVR (2007) Org Lett 9:1851
76. Zhao Y, Truhlar DG (2008) Acc Chem Res 41:157. doi:10.1021/ar700111a
77. Zhang X, Du H, Wang Z, Wu Y-D, Ding K (2006) J Org Chem 71:2862
78. Izquierdo M, Osuna S, Filippone S, Martín-Domenech A, Solá M, Martín N (2009) J Org Chem 74:1480
79. Wieczorek R, Dannenberg JJ (2008) J Phys Chem B 112:1320. doi:10.1021/jp077527j
80. Wieczorek R, Dannenberg JJ (2005) J Am Chem Soc 127:14534. doi:10.1021/ja053839t
81. Koblenz TS, Wassenaar J, Reek JNH (2008) Chem Soc Rev 37:247. doi:10.1039/b614961h
82. Clennan EL, Pace A (2005) Tetrahedron 61:6665. doi:10.1016/j.tet.2005.04.017
83. Natarajan A, Kaanumalle LS, Gibb SJ, Gibb BC, Turro NJ, Ramamurthy V (2007) J Am Chem Soc 129:4132. doi:10.1021/ja070086x
84. Greer A (2007) Nature 447:273. doi:10.1038/447273a
85. Chin KK, Trevithick-Sutton CC, McCallum J, Jockusch S, Turro NJ, Scaiano JC, Foote CS, Garcia-Garibay MA (2008) J Am Chem Soc 130:6912. doi:10.1021/ja800926v
86. Cojocaru B, Laferriére M, Carbonell E, Parvulescu V, García H, Scaiano JC (2008) Langmuir 24:4478. doi:10.1021/la800441n
87. Jockusch S, Sivaguru J, Turro NJ, Ramamurthy V (2005) Photochem Photobiol Sci 4:403. doi:10.1039/b501701g